Detection of the fungicide dodine via host-guest complexation between cucubit[10]uril and acridine orange

Cheng-hui Wang,[a] Hong-qian Zou,[a] Hang Cong,[a,b] Ying Huang,[a] Zhu Tao, Carl Redshaw,[c]* [a] Xin Xiao*[a]

[a] Key Laboratory of Macrocyclic and Supramolecular Chemistry of Guizhou Province, Guizhou University, Guiyang 550025, China.

[b] Enterprise Technology Center of Guizhou Province, Guizhou University, Guiyang 550025, China

[c] Department of Chemistry, University of Hull, Hull HU6 7RX, U.K.

E-mail: gyhxxiaoxin@163.com (X. Xiao), C.Redshaw@hull.ac.uk (C. Redshaw),

Abstract: The interaction between acridine orange (AO) and cucurbit[10]uril, Q[10] affords the ternary complex 2AO@Q[10]. Subsequent addition of dodine (DD) displaces AO from the Q[10] cavity, and results in a fluorescent output. The effect of 20 different pesticides, as well as a number of common interferents, on the fluorescent output is presented. Results revealed that the system is capable of the selective recognition of DD, with a limit of detection (LOD) for DD of 1.12×10^{-7} M.

Keywords: Cucurbit[10]uril; Acridine orange; Host-guest; Dodine

Introduction

Herbicides account for around 80% of all pesticide use, and have been extensively applied over the years against a variety of weed species. [1-3] However, with their use comes a range of toxicity issues, which can negatively impact on both the environment and human health. [4-8] Dodine (DD), 1-dodecylguanidinium acetate, is a generally used cationic surfactant, but also a protective and non-systemic fungicide. [9-10] In addition, DD also generally exists in industrial waste water and sewage, and has been extensively used in medical treatments, the chemical industry and for food packaging disinfection treatment. [11-12] Given the short UV absorption (200 nm) of DD, it is difficult to achieve the requirements of trace detection in high performance liquid chromatography [13-14], so the methods of residue analysis mainly include ion-pair high performance liquid chromatography [15] and high performance liquid chromatography-tandem mass spectrometry [16]. However, these techniques have complex sample pretreatment procedures, cumbersome operation, and require a large amount of organic solvent and long analysis time. Given this, there is a real need to develop systems that can readily detect DD at low concentrations. One potential method currently attracting attention is the use of macrocyclic systems that possess a cavity capable of readily encapsulating guests. [17-23] Cucurbit[*n*]urils (Q[*n*]s) are a relatively new class of macrocycle that have been shown to display rich host-guest chemistry [24-30]. The cavity of the Q[*n*] inside and outside is of different polarity, and when a compound is inside or outside the Q[*n*] cavity the fluorescence properties might well differ. By use of photochemical techniques, it is possible to sense or detect non-fluorescent or weakly fluorescent analytes [31-36]. Cucurbit[10]uril, Q[10], with its large cavity can selectivity include two guests, and the photochemical properties of such host-guest complexes allow for the sensing analytes such as metal ions, pesticides and drugs. With this in mind, we have recently exploited Q[10] for the detection of the fungicide DD. The approach involved a competitive interaction and the formation of a fluorescent turn-on system. [37-41] Herein, we investigate a related fluorescent turn-on system based on Q[10] for the detection of DD, which utilizes the dye acridine orange (AO) as the initial guest, see scheme 1.

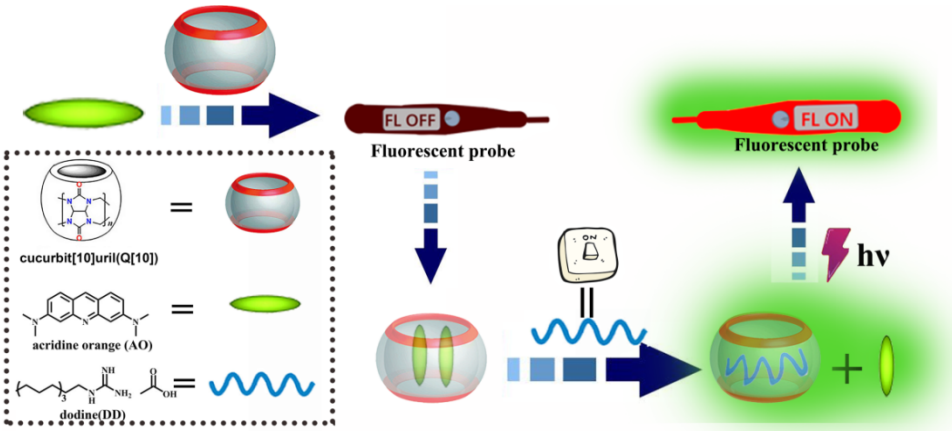

Scheme 1. Sensing behavior of 2AO@Q[10] probe toward DD.

Experimental

Materials

Acridine Orange (AO) was obtained from Aladdin (Shanghai, China). Q[10] was prepared and purified according to the literature method. [41] All pesticides used were obtained from commercial sources, and further purification was not necessary. Stock solutions of pesticides (1×10^{-3} mol/L), AO (1×10^{-3} mol/L) and Q[10] (1×10^{-5} mol/L) were prepared using double-distilled water. In addition, a variety of pesticides have been employed herein including Carbaryl (CAR), Acetamiprid (ATM), Triadimefon (TDF), Thiamethoxam (TTA), Dinotefuran (DFA), Pymetrozine (PTZ), Pyrimethanil (PMA), Paraquat (PQ), Hymexazol (HMZ), Azaconazole (ACZ), Flusilazole (FSZ), Mepronil (MEP), Carbendazim (CBZ), Bathocuproine (BCP), Napropamide (NPM), Fenoxaprop-ethyl (FE), Pyroquilon (PQL), Mefenacet (MN), Tebuconazole (TBZ), Penconazole (PCZ). The preparation process of the solutions employed herein was to dilute the stock solution to obtain the corresponding required concentration. This involved initially storing the stock standard solution at room temperature for several hours prior to use. When preparing the standard working solution, double distilled water was gradually dropped into the stock standard solution. All other chemicals were of analytical reagent grade.

^{1}H NMR spectroscopy

Experiments were recorded at 25 °C, using a JEOL JMM-ECZ400 spectrometer with D_2O as the field frequency lock. The observed chemical shift is reported in parts per million (ppm) relative to the built-in tetramethylsilane (TMS) standard (0.0 ppm).

UV-Vis absorption spectroscopy

The UV-vis absorption spectra of the host-guest complexes were recorded using an Agilent 8453 spectrophotometer at room temperature. The UV-vis absorption experiments were performed as follows: 100 μL of a 1×10^{-3} mol/L stock solution of AO and various amounts of an aqueous 1×10^{-5} mol/L Q[10] solution were transferred into a 10 mL volumetric flask, and then the volumetric flask was filled to the final volume with distilled water. Samples of these solutions were combined to give solutions with an $N_{Q[10]}/N_G$ = 0, 0.1, 0.2, 0.3, . ., and 1.0. The Job's plot method was used to determine the inclusion ratio of the substance, $N_G/(N_G + N_{Q[10]})$ = 0, 0.1, 0.2, 0.3, . . ., 1.0. The UV-vis absorption spectra of the solution were measured at room temperature after 2 h.

Fluorescence spectra

AO of concentration 1×10^{-5} mol/L was obtained by diluting the stock solution. A certain proportion of Q[10] solution was gradually added to free AO. The maximum emission wavelength (λ_{em}) of the sample is 540 nm, and the excitation wavelength (λ_{ex}) is 484 nm. The fluorescence emission spectra of the system were measured with a slit of 10 nm and an emission slit of 10 nm.

To the probe solution of the 2AO@Q[10] system (1×10^{-5} mol/L), 5 equiv. of pesticide solution (5×10^{-5} mol/L) was gradually added in proportions. Fluorescence spectra were obtained upon excitation at 484 nm (emission and excitation bandwidths: 10 nm) at room temperature, and the emission intensity was monitored at 540 nm.

To the probe solution of the 2AO@Q[10] system (1×10^{-5} mol/L), a certain amount of common ions and molecules in water and fruits and vegetables were added into the solution system. Fluorescence spectra were obtained upon excitation at 484 nm

(emission and excitation bandwidths: 10 nm) at room temperature, and the emission intensity was monitored at 540 nm. The fluorescence emission spectrum was measured according to the above method.

Limit of detection (LOD) measurement

The calculation technique used for the LOD was based on the standard derivation of 10 measurements without the guest molecule (σ) and the slope of the linear calibration curve (K) based on the formula LOD = 3σ/K. In the absence of guest molecules, the standard deviation for 10 measurements can be deduced using:$\sigma = \sqrt{\frac{1}{n-1}\sum_{i=1}^{n}(x_i - \bar{x})^2}$, where n is 11 measurements.

Results and discussion

The interaction between Q[10] and AO was monitored by ^{1}H NMR spectroscopy (Figure 1) in D_2O. It was evident from the upfield shifts of the proton signals (*versus* the free guest) that two AO guest molecules could be encapsulated within the Q[10] cavity, thereby forming an inclusion complex of the type 2AO@Q[10]. The presence of only a single set of resonances for AO suggested fast exchange of the ternary complex on the NMR timescale; a similar situation was observed for Q[10] and protonated acridine. [42]

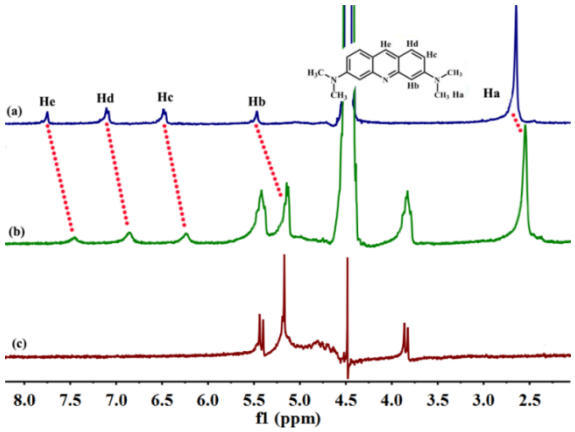

Figure 1. ^{1}H NMR spectra: (a) AO; (b) Q[10]: AO=1:2; (c) Q[10].

Spectral data were obtained in water at pH 5.6 (free pH value in the absence of buffer) working at dye concentrations of 10^{-5} mol/L. The interaction between Q[10] and AO was further studied using UV-vis spectroscopy. The free host Q[10] shows no

absorbance at λ > 210 nm. Figure 2 shows the variation in the UV spectra obtained for aqueous solutions containing a fixed concentration of AO and variable concentrations of Q[10]. The absorption maxima at 492 nm corresponded to the AO monomers. [43] Upon addition of Q[10] to the aqueous AO solution, the absorption band of the guest AO exhibits a decrease of the absorption peak at 492 nm with a blue shift to 466 nm. The spectral changes observed upon addition of Q[10] were due to the aggregation of AO and inclusion of dimer molecules in the Q[10] cavity. The data for absorbance (A) *vs*. the ratio of the number of moles (N) of the host Q[10] and guest AO can be fitted by a 2:1 binding model. Furthermore, a Job's plot (Figure 2c) confirmed the stoichiometry of the host-guest complex.

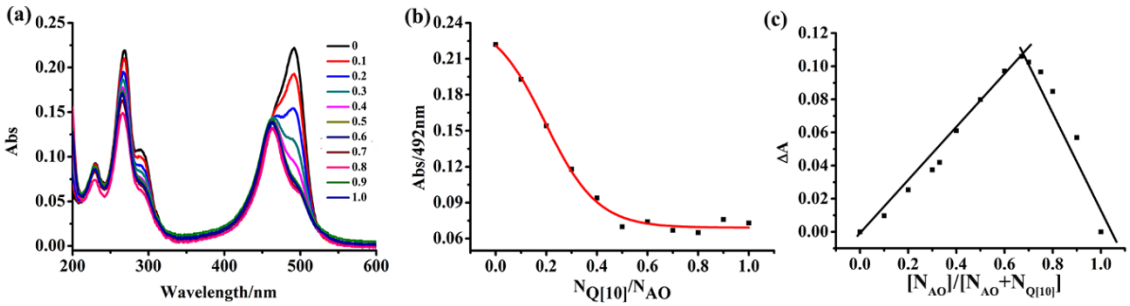

Figure 2. (a) UV-vis titration of AO (1.0×10^{-5} mol·L^{-1}) on increasing concentrations of Q[10]; (b) the concentrations and absorbance *vs*. $N_{Q[10]}/N_{AO}$ plots; (c) Continuous variation Job's plot for Q[10] and the guest on the basis of UV-vis titration spectra.

Fluorescence spectroscopy was further performed, and as shown in Figure 3, the strong fluorescence associated with AO in aqueous solution was quenched on addition of Q[10] (Figure 3a), and the titration curve (Figure 3b) fitted a 2:1 stoichiometry. It was found that under UV irradiation, the addition of 10 μM Q[10] afforded a dramatic change in the emission (Figure 3 inset). According to the previous UV-vis spectroscopic data and the ^{1}H NMR spectra, AO in the form of a dimer is encapsulated in the cavity Q[10]. The complexes formed by adding Q[10] were dimeric in nature and the self-quenching effect due to π-π interactions must be the reason for the decrease in fluorescence. [43]

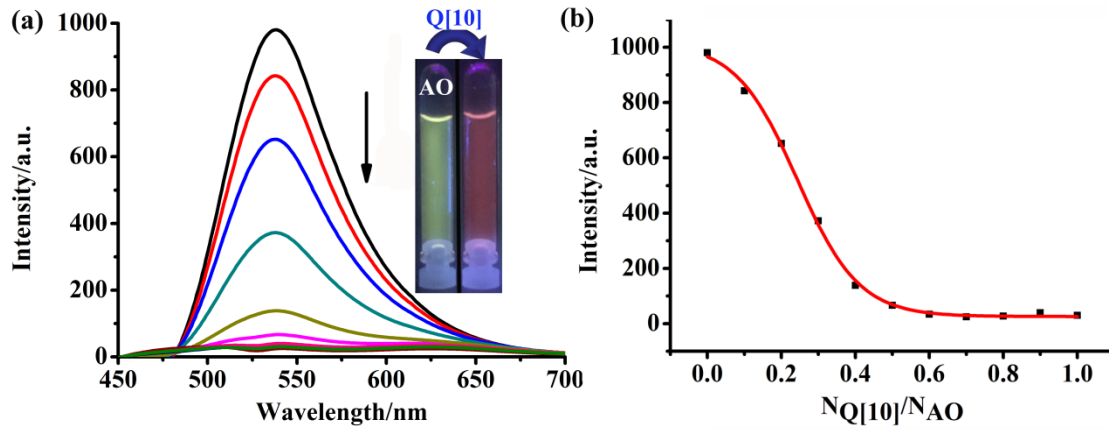

Figure 3. (a) Fluorescence spectra of AO (1.0×10^{-5} mol·L^{-1}) on increasing concentrations of Q[10] Ex. Wavelength: 484 nm, Ex. Slit:10 nm; inset: fluorescence color changes of AO solution before and after addition of Q[10] under illumination at 365 nm with a portable UV lamp; (b) the concentrations and intensity *vs*. $N_{Q[10]}/N_{AO}$ plots.

Given the results above, this system has the potential to be used for the detection of pesticides. Fluorescence experiments were performed with 20 common pesticides, including Carbaryl (CAR), Acetamiprid (ATM), Triadimefon (TDF), Thiamethoxam (TTA), Dinotefuran (DFA), Pymetrozine (PTZ), Pyrimethanil (PMA), Paraquat (PQ), Hymexazol (HMZ), Azaconazole (ACZ), Flusilazole (FSZ), Mepronil (MEP), Carbendazim (CBZ), Bathocuproine (BCP), Napropamide (NPM), Fenoxaprop-ethyl (FE), Pyroquilon (PQL), Mefenacet (MN), Tebuconazole (TBZ), Penconazole (PCZ), Dodine (DD), and it was observed (Figure 4) that only the use of DD afforded a pronounced fluorescent enhancement. From the titration spectra (Figure 5), a plot of fluorescence intensity *versus* $N_{DD}/ N_{2AO@Q[10]}$ revealed that the fluorescent enhancement (ΔI) has a linear correlation with DD concentration, and the limit of detection (LOD) for DD was 1.12×10^{-7} M.

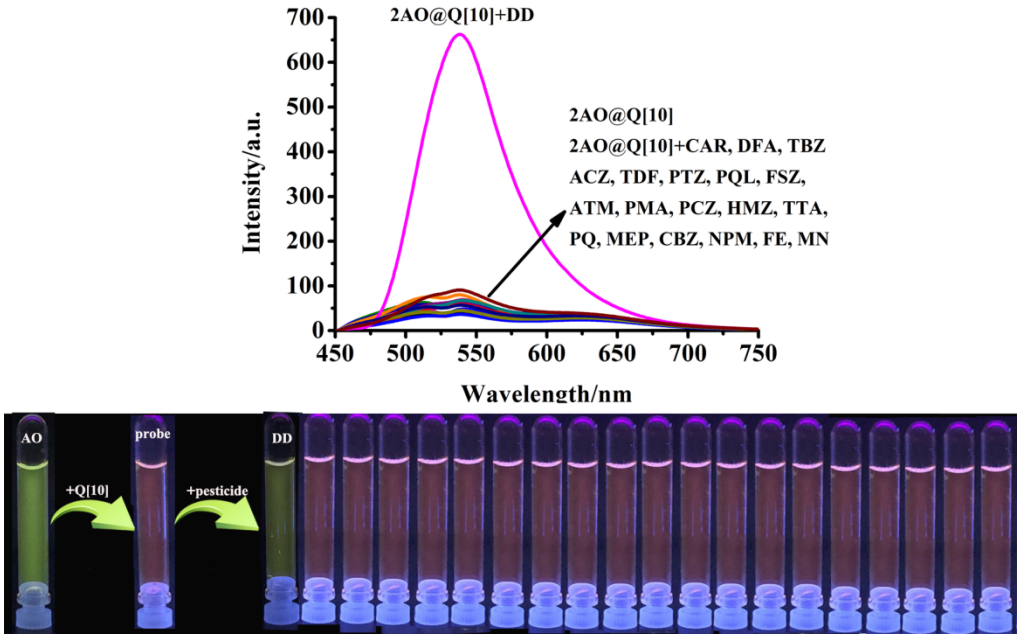

Figure 4. (top) The effect of 20 pesticides (5 equiv. of host–guest complex) on the relative fluorescence response (λ em = 540 nm) of 2AO@Q[10] (1.0×10^{-5} mol·L^{-1}) (2:1), Ex. Wavelength: 484 nm, Ex. Slit: 10 nm; (bottom) Photographs of 2AO@Q[10] systems containing 5 equiv. of host–guest complex and different 20 pesticides under exposure to UV light (365 nm).

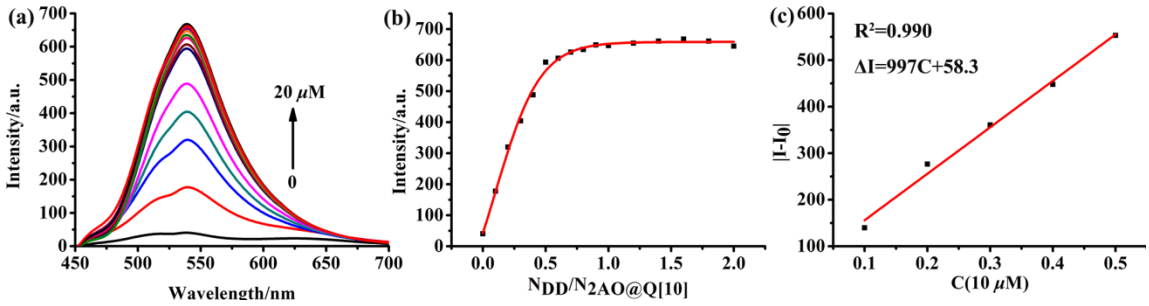

Figure 5. (a) Titration fluorescence spectra of 2AO@Q[10] (1.0×10^{-5} mol·L^{-1}, 2:1) upon addition of increasing amounts dodine (0, 0.1, 0.2……0.9, 1.0, 1.2, 1.4……1.8, and 2.0 equiv.); (b) Plots of $N_{Dodine}/N_{2AO@Q[10]}$, (c) Non-linear fitting curves for changes in the fluorescence intensity of the inclusion complex in the presence of different concentrations of dodine.

Table 1. Standard deviation and detection limit calculation for DD

Fluorescence Intensity	Standard deviation(σ)	Slope(K)	Detection limit(3σ/K)
144.5917			
146.2517			
140.7159			
138.1885			
140.2242			
139.9547	3.73	997×10^6 M^{-1}	1.12×10^{-7} M
135.4037			

137.1586
133.4779
134.7138
139.4833

In acidic or neutral solutions, AO mainly exists in the protonated form, and the absorption peak at 492 nm is the main absorption peak, while in alkaline solutions, AO mainly exists in the un-protonated form, and the original main absorption peak was blue shifted to 435 nm (Figure 6a). From the p*K*a titration curve, the p*K*a of AO is about 9.7 (Figure 6b). From the fluorescence emission spectra of AO at different pH values (Figure 7), it was also observed that over the pH range 2-9, the fluorescence intensity of AO at 540 nm does not change. However, when the pH>9, the fluorescence intensity emission decreases significantly, and by fitting the p*K*a titration curve, the p*K*a of AO is about 9.7. This is consistent with UV-vis spectral data.

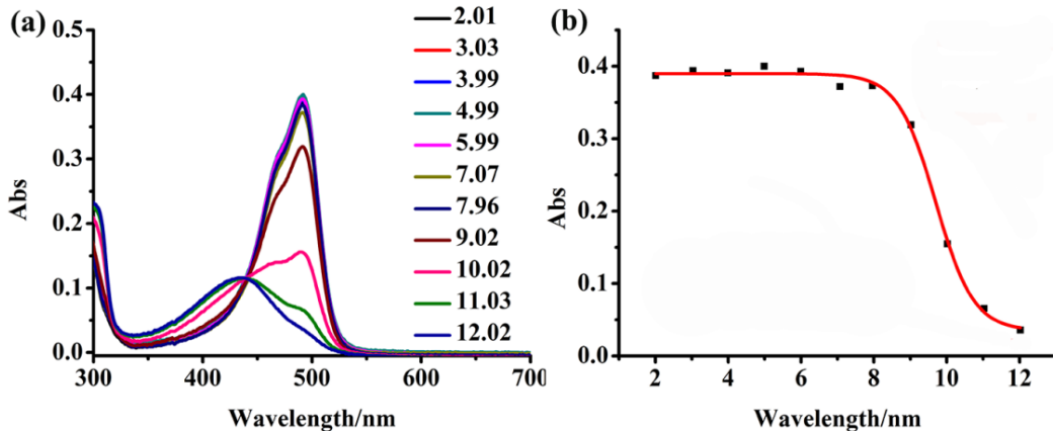

Figure 6. (a) UV-Vis absorption of AO (1.0×10^{-5} mol•L^{-1}) at different pH in Tris-HCl; (b) The variation in absorbance with pH at 492 nm in Tris-HCl.

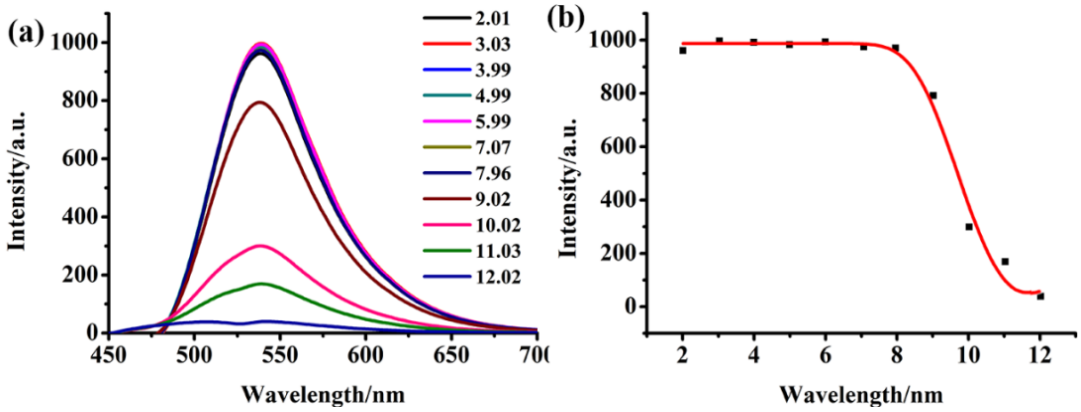

Figure 7. (a) Fluorescence absorption of AO (1.0×10^{-5} mol•L^{-1}) at different pH in Tris-HCl (λ ex＝484 nm); (b) plots of fluorescence absorption at 540 nm for AO at various pHs.

The system has also been evaluated for its efficiency when operating in the presence of common interferents such as metal ions and common interferences. The results (Figure 8, Table 1) revealed that in the presence of DD, the interferents tested had little impact on the observed fluorescence intensity.

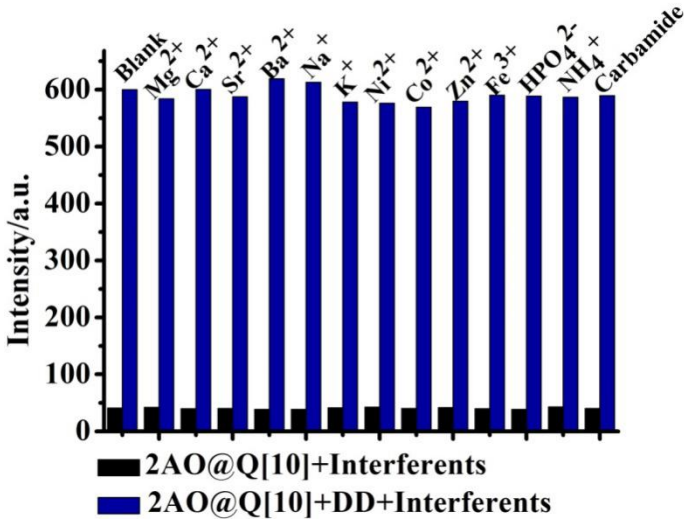

Figure 8. Fluorescence intensity changes of 2AO@Q[10] (1.0×10^{-5} mol•L^{-1}) and 2AO@Q[10]＋DD (1.0×10^{-5} mol•L^{-1}) with different interferents (λex＝484 nm).

Table 2 Results of the selectivity study

Complex	Other Interferents	Interference
2AO@Q[10]+DD	Ba^{2+} Co^{2+} Fe^{3+}	100
	K^{+}	150
	Ca^{2+}, Ni^{2+}, Zn^{2+}	200
	HPO_4^{2-}	250
	Sr^{2+}, Mg^{2+}, Na^{+}	300
	NH_4^{+}, Carbamide	400

To shed further light on the recognition process involving DD and the 2AO@Q[10] complex, the addition was carried out in D_2O and monitored by ^1H NMR spectroscopy. Following gradual addition of DD (Figure 9), the proton resonances associated with the guest AO shifted downfield ($H_a = 0.11$; $H_b = 0.22$; $H_c = 0.22$; $H_d = 0.22$; $H_e = 0.27$ ppm), which suggested that these protons are being removed from the Q[10] cavity. Meanwhile, the DD protons (H_1, H_2, H_3 and H_4) experienced an upfield shift relative to

free DD. These observations further demonstrated that the included AO guest was displaced by the DD molecule in the cavity of the Q[10].

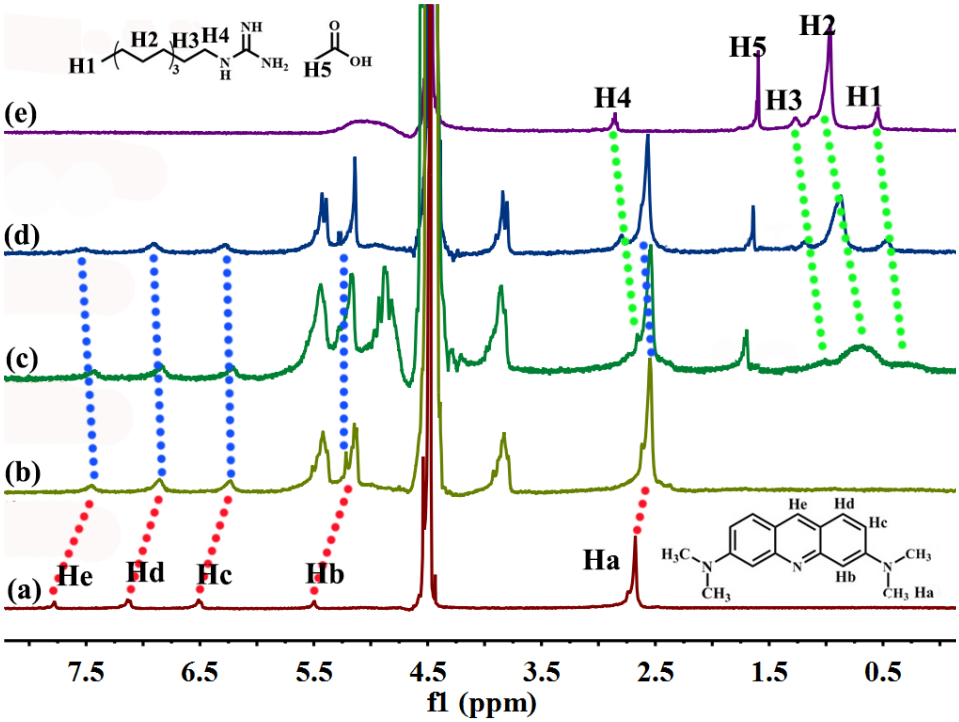

Figure 9. ^{1}H NMR spectra obtained from the titration of AO with Q[10]: (a) AO; (b) Q [10]:AO=1:2; (c) Q[10]:AO:DD=1:2:1; (d) Q[10]:AO:DD=1:2:2; (e) DD.

Conclusion

In this report, we have constructed a probe using the dye acridine orange (AO) and cucurbit[10]uril (Q[10]), which is capable of the selective detection of dodine (DD). The probe operates by a competitive displacement process, whereby added DD displaces two AO guests from the Q[10] cavity. This displacement means that the fluorescence of the AO is no longer quenched by the Q[10], and an obvious fluorescent signal is achieved. We propose this supramolecular system can be not only extended to identify DD fluorescent probes with long-wavelength emission but also expanded to other platforms/applications such as cell imaging, drug delivery and textile dyeing.

ACKNOWLEDGEMENTS

This work was supported by the Science and Technology Department of Guizhou Province (Grant No. ZK-2021-024), the National Natural Science Foundation of China (No. 22061009) and the Innovation Program for High-level Talents of Guizhou Province (No. 2016-5657). CR thanks the EPSRC for an Overseas Travel Grant (EP/R023816/1).

References

[1] S. A. Levin, *Elsevier Inc*. **2013**, 87-95.

[2] D. L. Shaner, Pest Manag. Sci. **2000**, *56*, 320-326.

[3] G. Schütte, M. Eckerstorfer, V. Rastelli, W. Reichenbecher, S. Restrepo-Vassalli, M. Ruohonen-Lehto, M. Mertens, *Environ. Sci. Eur*. **2017**, *29*, 1-12.

[4] W. Boedeker, M. Watts, P. Clausing, E. Marquez, *BMC Public Health* **2020**, *20*, 1-19.

[5] P. C. Ray, H. Yu, P. P. Fu, *J. Environ. Sci. Heal. C* **2009**, *27*, 1-35.

[6] J. N. Hahladakis, C. A.Velis, R. Weber, E. Iacovidou, P. Purnell, *J. hazard. Mater*. **2018**, *344*, 179-199.

[7] L. Rani, K. Thapa, N. Kanojia, N. Sharma, S. Singh, A. S. Grewal, J. Kaushal, *J. Clean. Prod*. **2021**, *283*, 124657.

[8] P. Kiddee, R. Naidu, M. H. Wong, *Waste manage*. **2013**, *33*, 1237-1250

[9] L. V. Evans, M. E. Callow, K. R. Wood, *Studies. Environmental. Science.* Elsevier, **1986**, *28*, 55-64.

[10] Y. M. Lim, H. Kim, S. K. Lim, J. Yoo, J. Y. Lee, I. C. Eom, B. I. Yoon, P. Kim, S. D. Yu, I. Shim, *Toxics* **2020**, *8*, 76-92.

[11] B. Srivastava, V. Jhelum, D. D. Basu, P. K. CSIR, **2009**, *28*, 839-850.

[12] Y. Zhang, J. L. Zhou, *Water res.* **2005**, *39*, 3991-4003.

[13] J. P. S. Cabral, A. R. W. Smith, *J. Colloid Interf. Sci*. **1992**, *149*, 27-33

[14] T. Kovalczuk, O. Lacina, M. Jech, J. Poustka, J. Hajšlová, *Food addit. contam. B* **2008**, *25*, 444-457

[15] N. K. Karamanos, P. Vanky, G. N. Tzanakakis, T. Tsegenidis, A. Hjerpeb. *J.*

Chromatogr. A **1997**, *765*, 169-179.

[16] C. L. Hetherton, M. D. Sykes, R. J. Fussell, D. M. Goodall., *Rapid Commun. Mass Sp*. **2004**, *18*, 2443-2450

[17] K. Ariga, T. Kunitake, *Springer Science & Business Media* **2006**.

[18] B. D. Wagner, *De Gruyter*, **2020**.

[19] D. Yang, M. Liu, X. Xiao, Z. Tao, C. Redshaw, *Coord. Chem. Rev*. **2021**, *434*, 213733.

[20] C. Sun, Z. Wang, L. Yue, Q. Huang, Q. Cheng, R. Wang, *J. Am. Chem. Soc*. **2020**, *142*, 16523-16527.

[21] K. Yang, G. Yu, Z. Yang, L. Yue, X. Zhang, C. Sun, J. Wei, L. Rao, X. Chen, R. Wang, *Angew. Chem. Int. Ed*. **2021**, *60*, 17570-17578.

[22] S. Guo, Q. Huang, Y. Chen, J. Wei, J. Zheng, L. Wang, Y. Wang, R. Wang, *Angew. Chem. Int. Ed*. **2021**, *60*, 618-623.

[23] M. Liu, Y. Zhou, Li. Chen, B. Bian, X. Xiao, Z. Tao, *Chinese Chem. Lett*. **2021**, *32*, 375 – 379.

[24] H. Wu, J. Zhao, X. N. Yang, D. Yang, L. X. Chen, C. Redshaw, L. G. Yang, Z. Tao, X. Xiao, *Dyes Pigments* **2022**, *199*, 110076.

[25] W. Zhang, Y. Luo, J. Zhao, W. H. Lin, X. L. Ni, Z. Tao, X. Xiao, C. D. Xiao, *Sensors and Actuat B-Chem*. **2022**, *354*, 131189.

[26] M. Liu, L. X. Chen, P. H. Shan, C. Lian, Z. Zhang, Y. Zhang, Z. Tao, X. Xiao, *ACS Appl. Mater. Inter*. **2021**, *13*, 7434-7442.

[27] M. Liu, M. Yang, Y. Yao, Y. Zhang, Y. Zhang, Z. Tao, Q. Zhu, G. Wei, B. Bian, X. Xiao, *J. Mater. Chem. C*. **2019**, *7*, 1597-1603.

[28] M. Liu，J. Kan, Y. Yao, Y. Zhang, B. Bian, Z. Tao, Q. Zhu, X. Xiao, *Sensor Actuat B: Chem*. **2019**, *283*, 290-297.

[29] R. H. Gao, L. X. Chen, K. Chen, Z. Tao, X. Xiao, *Coord. Chem. Rev*. **2017**, *348*, 1-24.

[30] C. Márquez, R. R. Hudgins, W. M. Nau, *J. Am. Chem. Soc*. **2004**, *126*, 5806-5816.

[31] Luo Y, Zhang W, Yang M X, X. H. Feng, C. Redshaw, Q. Li, Z. Tao, X. Xiao, *Macromolecules* **2022**, *55*, 1642-1646.

[32] R. Cen, M. Liu, J. Lu, W. Zhang, J. Dai, X. Zeng Z. Tao, X. Xiao, *Chinese Chem.*

Lett. **2022**, *33*, 2469 – 2472.

[33] Zhang W, Luo Y, J. Zhao, C. Zhang, X. L. Ni, Z. Tao, X. Xiao, *Chinese Chem. Lett*. **2022**, *33*, 2455 – 2458.

[34] P. H. Shan, J. Zhao, X. Y. Deng, R. L. Lin, B. Bian, Z. Tao, X. Xiao, J. X. Liu, *Anal. Chim. Acta*. **2020**, *1104*, 164-171.

[35] X. Y. Zhu, X. N. Yang, H. Wu, Z. Tao, X. Xiao, *B. Chem. Soc. Jpn*. **2022**. (doi.org/10.1246/bcsj.20210332).

[36] Y. Luo, W. Zhang, M. Liu, J. Zhao, Y. Fan, B. Bian, Z. Tao, X. Xiao, *Chinese Chem. Lett*. **2021**, *32*, 367-370.

[37] H. Feng, Y. Luo, M. Liu, Q. Chen, Z. Tao, X. Xiao, *New J. Chem*. **2021**, *45*, 22133-22140.

[38] J. Li, K. Chen, L. Zhu, X. Li, C. Li, Q. Chang, W. Xu, *Front. Chem*. **2022**, *10*, 856698.

[39] J. Yang, S. W. Chen, B. Zhang, Q. Tu, J. Wang, M. S. Yuan, *Talanta* **2022**, 123200.

[40] Z. Li, J. R. Askim, K. S. Suslick, *Chem. Rev*. **2018**, *119*, 231-292.

[41] Y. Yu, Y. Li, X. Wang, H. Nian, L. Wang, J. Li, Y. Zhao, X. Yang, S. Liu, L.Cao, *J. Org. Chem*. **2017**, *82*, 5590-5596.

[42] W. T. Xu, Y. Luo, W. W. Zhao, M. Liu, G. Y. Luo, Y. Fan, R. L. Lin, Z. Tao, X. Xiao, J. X.; Liu, *J. Agr. Food Chem.* 2021, *69*, 584-591.

[43] P. Montes-Navajas, A. Corma, H. Garcia, *ChemPhysChem*, **2008**, 9, 713-720.